Numerical Investigation of Non-linear Radiation Effects in Boundary Layer Oblique Stagnation Point Flow of non-Newtonian Fluids over a Symmetrically Stretching Surface under the Effects of Magnetic Field

Bilal Ahmed[1,*], M. Noman[1] A. Aqsa[1] and S. Kanwal[1]

[1]Department of Mathematics and Statistics, The University of Lahore, Pakistan

*****Correspondence: bilalmaths7@yahoo.com*

Abstract: The numerical solution of the flow of non-Newtonian fluid induced by symmetrically stretching fractal sheet in the region of oblique stagnation point flow under the inducement of externally applied uniform magnetic field orthogonal to the flow is presented. The analysis is made under the assumption of a boundary layer which arrives at the system of partial differential equations which afterward is transformed into ordinary differential equations by using appropriate similarity transformations. The numerical solution of the modeled system of equation is obtained by parallel shooting technique and then presented for different variations of involved parameters. It is noted that enhancement in the magnetic field results in a decrease in horizontal velocity and the boundary layer becomes thinner. The behavior of streamlines shows that the symmetry of the flow is highly dependent on the obliqueness of the stagnation point flow. It is seen that when the ratio of $a/c>1$, the flow has a normal boundary layer structure but when $a/c<1$ then the structure shows inverted behavior. It is also seen that there exists no boundary layer when $a/c=1$. The obtained results are also compared with the available results in the literature and found in excellent agreement in the limiting cases.

Keywords: Thermal radiation; uniform magnetic field; boundary layer; Maxwell fluid; oblique stagnation point

1. Introduction

When a fluid reaches the stagnation point, its local velocity becomes zero. The surface of the body exists in the flow at fluid stagnation point, and the fluid of the body is at rest. The oblique stagnation point flow discussed and combined at a plane wall are free restriction positions. Stagnation point flow at oblique flow consists of an orthogonal flow to which an infinite velocity is added. When a fluid collides with a surface, its velocity vanishes, or becomes zero, this is referred to as a stagnation point. Recently many researchers have been taking extra interest in stagnation point flows due to numerous applied applications in different industries. Cooling of nuclear reactors is an example of stagnation flow. In stagnation flow, the attention-able thing is that the greatest heat moves, and pressure gradient is found at stagnation stage. Initially Stuart [1] worked on stagnation flow obtained the analytical solutions for the flow. Tamada [2] and Dorrepaal [3] were the first who generalize the flow involving stagnation point and obtained solution for oblique stagnation point. In their study, Tooke and Blyth [4] conducted a concise examination of oblique stagnation point flow. Their findings revealed that, in the presence of significant adverse pressure gradients, there exists a region near the wall where the shear component experiences reversed flow. Interestingly, the integration of orthogonal flow with shear flows, each exhibiting varying degrees of reversed flow, consistently results in the same oblique flow pattern. However, the attachment point of stagnation is predictably displaced along the wall. Husain et al. [5] worked on continuous the work viscoelastic fluid model in stagnation point flow.

The non-Newtonian fluid model is more difficult and complex to solve the individual constitutive equation, but the Newtonian fluid model is easy to solve the constitutive equation. Moreover, the purpose of much research describes their application, Maxwell finds the proposal attention to the simplicity of viscoelastic fluid. Wang and Tan [6] studied the linear stability explanation by the Maxwell fluid model with the thermal diffusion effect. Mukhopadhyay [7] and Nadeem et al. [8] provided more generalized literature. The most important stretching surface used by industrial firms, such as warm progression, metal sheet freezing, crystal fibers, wire drawing, and various other materials. The oscillatory convection damaged the system by thermal diffusion and undependability of the rise system due to increase time composure. Bilal et al. [9] the three combined convection radiative flow of non-Newtonian fluid over an inclined stretching surface in the presence of thermophoresis and the condition is convective. Javed et al. [10] noticed that Maxwell fluid is the more suggested flow of stagnation point comprehensively. Tariq et al. [11] study the numerical analysis mixed convection boundary layer flow second grand viscoelastic due to cylinder of the elliptic cross section with prescribed surface heat flux.

A flow model solves the boundary layer approximation by a non-linear equation like continuous and momentum transformation. Sajid et al. [12] analyzed the heat transfer in the stagnation - point flow of a Jeffrey fluid elapsed lubricant to reduce friction and wear and tear in contact between two surfaces. Khan et al. [13] generalized diffusion effects on Maxwell nanofluid stagnancy point flow over an extended sheet with chemical reaction in slip conditions. Jawad et al. [14] studied the partition of Non-linear thermal radiation and the sticky carelessness effect on the time-independent rotating in the three-dimensional flow of single-wall carbon nanotubes with sedimentary suspensions. Majeed et al. [15] studied the influence of rotating the magnetic field on Maxwell concentrated ferrofluid flow over a heated widening sheet with heat generation. Khalid et al. [16] heat transfer in the flow of Jeffrey fluid past a lubricated surface near a stagnation point flow. Rasool et al. [17] the magnetic field and effects of radiation of stagnation point flow on mixed convection flow of a cylinder under local thermal non-equilibrium in a porous medium. Reza-E-Rabbi et al. [18] the fluid flow behavior over a stretching sheet computational modeling of multiphase radiative Casson and maxwell fluid the appearance of nano-size particles.

Khan et al. [19] the analysis mixed convection flow of Maxwell fluid as the combination of both coupled free and force convection between two infinite stretching disks with the source of heat. This paper investigates the problem of oblique hydromagnetic stagnation flow of point an electrically

Casson fluid over a stretching sheet embedded in a doubly stratified medium in the presence of heat source and thermal radiation with the first chemical reaction. Ibrahim et al. [20] presented study slipped effect on stagnation point flow of upper converted non-Newtonian fluid of nanofluid passing a stretching sheet with chemical reaction. Mekheimer and Ramadan [21] provided the study about the perspectives on gyrotactic microorganisms in the context of bio-thermal convection of Prandtl nanofluid over a permeable sheet subjected to stretching or shrinking and revealed that temperature and density of motile microorganisms are elevated when a shrinking sheet is considered, in contrast to the case of a stretching sheet.

Chu et al [22] investigated the heat and mass transfer in hydromagnetic stagnation point flow and provide the dual solution for the Carreau nanomaterial using Runge-Kutta Fehlberg method and concluded that velocity of fluid is raised for both solution by raising the intensity of suction parameter. Khan et al. [23] presented the numerical solution of the stagnation point flow of non-Newtonian fluid Cattaneo-Chirstov heat flux model and deduced that magnitude of drag force or velocity gradient increases via increase in the strength of applied magnetic field. Mathew et al. [24] considered multi slip and nanoparticle shape to analysis the stagnation point flow of silver blood fluid. Stagnation point flow and heat transfer analysis over stretching surfaces like plates and cylinders are addressed by Turkyilmazoglu [25]. He evaluated the exact solution for the flow modeled equations and deduced from the solution that heat transfer rates from the surfaces in both flow geometries are enhanced by the action of walls, with more cooled surfaces in the presence of wall suction. Zaheer et al. [26] investigated Electroosmotic Forces Driving Boundary Layer Flow of a Non-Newtonian Fluid Containing Planktonic Microorganisms Using the Darcy-Forchheimer Model and concluded that In comparison to a Newtonian fluid, the boundary layer velocity is reduced when dealing with a non-Newtonian fluid. However, the presence of the electro-osmotic parameter causes an increase in boundary layer velocity.

Abbasi et al. [27] gave the outcomes about the impacts of nonlinear warm radiation for axisymmetric rotational stagnation point stream with initiation energy and referenced that hub speed increments while auxiliary speed diminishes by expanding the turn boundary. Wahid et al. [28] looked into the MHD stagnation-point flow of nanofluid caused by a shrinking sheet with melting, viscous dissipation, and Joule heating effects. They recommended that the concentrate likewise proposes considering 2% of alumina volume part rather than 1% so the stream detachment interaction can be postponed, and at the same time support the laminar stream. At a certain level of shrinkage, the increased melting effect reduces skin friction by approximately 5%. Reddy et al. [29] reasoned that an increase in the Prandtl number results in a reduction in the temperature profile when they examined the vehicle properties of the stagnation point stream of hydro-attractive radiative nanofluid on the extending surface. Baig et al. [30] examined the precise solution of stagnation point flow on a nanofluid cylinder in the presence of ambient heat. Their research revealed that stagnation flow prevails over stretching flow at higher oncoming pressure flow values. Most of the published research on stagnation point flow uses numerical methods to explain the subject, but the goal of their study is to provide a precise solution to the issue at hand. Gadelhak et al. [31] provide the Numerical Analysis of Energy Transport in Williamson Nanofluid Flow over a Curved Stretching Surface Using Finite Difference Method (FDM) and deduced that the heat flux decreases as the curvature parameter attains higher values further down. Additionally, both the Sherwood number and Schmidt number increase with higher values of the curvature parameter.

Many analyses show that the study of two-dimensional boundary layer stagnation point flows is interesting in the analysis of fluid flow and heat transfer over a stretching sheet. The basis for this is that these kinds of research have been used in the manufacturing sector. The creation of glass fiber, hot rolling, continuous casting, extrusion, manufacture of sheets, coating, and production of paper are examples of manufacturing processes. In the present problem, the study of boundary layer oblique stagnation point flow of Maxwell fluid with radiation effects over a linear stretching sheet under the inducement of the magnetic field has been carried out which has not been studied yet. The mathematical modeling based on Tooke and Blyth [4] and numerical simulation using the parallel shooting technique of governing equations are presented. The effects of different involved parameters on heat and fluid flow are presented through tables and graphs and a detailed discussion is given in the later part of the manuscript. An excellent agreement of results has been found with Pop et al. [32] and Javed and Ghaffari [10].

2. Problem Formulation

Consider the two-dimensional steady flow of Maxwell fluid over a stretching sheet in the region of non-orthogonal stagnation point under the influence of externally applied uniform magnetic field orthogonal to the flow. The stretching sheet is assumed along the plane $y=0$ and the flow moves along the $y-$axis. The velocity $U_w = cx$ is the stretching velocity of the sheet, with $c(>0)$ being the stretch constant as shown in Figure 1. The governing equations in the presence of body forces that describes the current flow are,

$$div\bar{V} = 0, \tag{1}$$

$$\rho \frac{d\bar{V}}{dt} = -\nabla p + div\bar{S} + \rho b, \tag{2}$$

$$\bar{u}\frac{\partial \bar{T}}{\partial \bar{x}} + \bar{v}\frac{\partial \bar{T}}{\partial \bar{y}} = \frac{k}{\rho c_p}\bar{\nabla}^2\bar{T} - \frac{1}{\rho c_p}\bar{\nabla}.q_r, \tag{3}$$

The div characterizes the divergence operator, $\bar{V} = [\bar{u}, \bar{v}, 0]$ is the vector velocity, $\bar{u}$ and $\bar{v}$ are the velocity movement components in the direction of $\bar{x}$ and $\bar{y}$ axis respectively. The bar shows that these quantities are in dimensionless form that will be converted into dimensional form where ρ is the density, p is the pressure, κ is the thermal conductivity fluid, c_p is the steady pressure of real heat, b is the is the body force caused by the magnetic field and q_r represents the radiative heat flux and $\bar{S}$ is the extra stress tensor for Maxwell fluid is explain below,

$$q_r = -\frac{4\sigma^*}{3(\alpha_r + \sigma_s)} \nabla \bar{T}^4, \tag{4}$$

$$\bar{S} + \lambda_1 \frac{D\bar{S}}{Dt} = \mu \bar{A}_1, \tag{5}$$

where Stefan Boltzmann's-constant is σ^* while α_r, σ_s, μ, and λ_1 the Rosseland definition is the corresponding fluid for dynamic viscosity, scattering coefficient, absorption coefficient, and time relaxation content. $\bar{A}_1$ is the representation of the first tensor by Rivlin Ericksen, explained by,

$$\bar{A}_1 = \bar{L} + \bar{L}^T. \tag{6}$$

The of velocity gradient and its transpose are represented by $\bar{L}$ and $\bar{L}^T$ respectively which are defined as,

$$\bar{L} = \begin{pmatrix} \frac{\partial \bar{u}}{\partial \bar{x}} & \frac{\partial \bar{u}}{\partial \bar{y}} & 0 \\ \frac{\partial \bar{v}}{\partial \bar{x}} & \frac{\partial \bar{v}}{\partial \bar{y}} & 0 \\ 0 & 0 & 0 \end{pmatrix} \text{ and } \bar{L}^T = \begin{pmatrix} \frac{\partial \bar{u}}{\partial \bar{x}} & \frac{\partial \bar{v}}{\partial \bar{x}} & 0 \\ \frac{\partial \bar{u}}{\partial \bar{y}} & \frac{\partial \bar{v}}{\partial \bar{y}} & 0 \\ 0 & 0 & 0 \end{pmatrix}. \tag{7}$$

The D/Dt is an operator explained correspondingly in the form of a contravariant vector and contravariant tensor of rank 2 in Eq. (8) and (9) respectively.

$$\frac{D\bar{S}}{Dt} = \frac{dS}{dt} - \bar{L}\bar{S}, \tag{8}$$

$$\frac{D\bar{S}}{Dt} = \frac{dS}{dt} - \bar{L}\bar{S} - \bar{S}\bar{L}^T. \tag{9}$$

Divergence applied on Eq. (5) yields,

$$\left(1 + \lambda_1 \frac{D}{Dt}\right) \nabla . S = \mu \nabla . \bar{A}_1. \tag{10}$$

Application of $\left(1 + \lambda_1 \frac{D}{Dt}\right)$ on both sides of Eq. (2) yields,

$$\left(\rho \frac{d\bar{V}}{dt} + \nabla p\right)\left(1 + \lambda_1 \frac{D}{Dt}\right) = \left(1 + \lambda_1 \frac{D}{Dt}\right) div\bar{S} + \left(1 + \lambda_1 \frac{D}{Dt}\right)\rho b, \tag{11}$$

$$\therefore divS = \nabla . S. \tag{12}$$

So,

$$\left(\rho\frac{d\bar{V}}{dt}+\nabla p\right)\left(1+\lambda_1\frac{D}{Dt}\right)=\left(1+\lambda_1\frac{D}{Dt}\right)\nabla.S+\left(1+\lambda_1\frac{D}{Dt}\right)\rho b, \tag{13}$$

The body fore defined in the above equation represents the Lorentz force which can be expressed as,

$$b^i=\sigma\left[\bar{V}\times\bar{B}\right]\times\bar{B}\,. \tag{14}$$

As flow is the $x-$direction and B_0 is the strength of uniform constant magnetic field that applied in $y-$direction, therefore we have,

$$\bar{B}=\left(0,B_0,0\right). \tag{15}$$

Thus

$$\bar{V}\times\bar{B}=\left(0,0,uB_0\right)$$

and

$$\left(\bar{V}\times\bar{B}\right)\times\bar{B}=\left(-uB_0^2,0,0\right). \tag{16}$$

Using Eq. (16) in Eq. (14) yields,

$$div\bar{V}=0, b^i=\left(-\sigma uB_0^2,0,0\right). \tag{17}$$

Using Eq. (17) in Eq. (13) and then expressed in component form,

$x-$component,

$$\left(\bar{u}\frac{\partial\bar{u}}{\partial\bar{x}}+\bar{v}\frac{\partial\bar{u}}{\partial\bar{y}}\right)=-\frac{1}{\rho}\frac{\partial p}{\partial\bar{x}}-\frac{\lambda_1}{\rho}\left(\bar{u}\frac{\partial^2 p}{\partial\bar{x}^2}+\bar{v}\frac{\partial^2 p}{\partial\bar{x}\partial\bar{y}}-\frac{\partial\bar{u}}{\partial\bar{x}}\frac{\partial p}{\partial\bar{x}}-\frac{\partial\bar{u}}{\partial\bar{y}}\frac{\partial p}{\partial\bar{y}}\right)+v\left(\frac{\partial^2\bar{u}}{\partial\bar{x}^2}+\frac{\partial^2\bar{u}}{\partial\bar{y}^2}\right)$$
$$-\lambda_1\left(\bar{u}^2\frac{\partial^2\bar{u}}{\partial\bar{x}^2}+2\overline{uv}\frac{\partial^2\bar{u}}{\partial\bar{x}\partial\bar{y}}+\bar{v}^2\frac{\partial^2\bar{u}}{\partial\bar{y}^2}\right)-\sigma uB_0{}^2+\lambda_1\left(-\sigma B^2{}_0 v\frac{\partial u}{\partial y}\right), \tag{18}$$

$y-$component,

$$\left(\bar{u}\frac{\partial\bar{v}}{\partial\bar{x}}+\bar{v}\frac{\partial\bar{v}}{\partial\bar{y}}\right)=-\frac{1}{\rho}\frac{\partial p}{\partial\bar{y}}-\frac{\lambda_1}{\rho}\left(\bar{v}\frac{\partial^2 p}{\partial\bar{y}^2}+\bar{u}\frac{\partial^2 p}{\partial\bar{x}\partial\bar{y}}-\frac{\partial\bar{v}}{\partial\bar{x}}\frac{\partial p}{\partial\bar{x}}-\frac{\partial\bar{v}}{\partial\bar{y}}\frac{\partial p}{\partial\bar{y}}\right)+v\left(\frac{\partial^2\bar{v}}{\partial\bar{x}^2}+\frac{\partial^2\bar{v}}{\partial\bar{y}^2}\right)$$
$$-\lambda_1\left(\bar{u}^2\frac{\partial^2\bar{v}}{\partial\bar{x}^2}+\overline{2uv}\frac{\partial^2\bar{v}}{\partial\bar{x}\partial\bar{y}}+\bar{v}^2\frac{\partial^2\bar{v}}{\partial\bar{y}^2}\right)+\lambda_1\left(\sigma B^2{}_0 u\frac{\partial v}{\partial x}\right). \tag{19}$$

The boundary conditions discussed by Javed and Ghaffari [10] are given below in the present flow problem are,

$$\left.\begin{array}{lll}\bar{u}=\overline{cx},\ \bar{v}=0, & \text{at} & \bar{y}=0\\ \bar{u}=a\bar{x}+b\bar{y}, & \text{as} & \bar{y}\to\infty,\end{array}\right\} \tag{20}$$

.

Eqs. (19) and (20) reduced by using boundary layer approximation as follows,

$$\left(\bar{u}\frac{\partial \bar{u}}{\partial \bar{x}}+\bar{v}\frac{\partial \bar{u}}{\partial \bar{y}}\right)=-\frac{1}{\rho}\frac{\partial p}{\partial \bar{x}}-\frac{\lambda_1}{\rho}\left(\bar{u}\frac{\partial^2 p}{\partial \bar{x}^2}+\bar{v}\frac{\partial^2 p}{\partial \bar{x}\partial \bar{y}}-\frac{\partial \bar{u}}{\partial \bar{x}}\frac{\partial p}{\partial \bar{x}}-\frac{\partial \bar{u}}{\partial \bar{y}}\frac{\partial p}{\partial \bar{y}}\right)+\nu\left(\frac{\partial^2 \bar{u}}{\partial \bar{x}^2}+\frac{\partial^2 \bar{u}}{\partial \bar{y}^2}\right)$$
$$-\lambda_1\left(\bar{u}^2\frac{\partial^2 \bar{u}}{\partial \bar{x}^2}+2\bar{u}\bar{v}\frac{\partial^2 \bar{u}}{\partial \bar{x}\partial \bar{y}}+\bar{v}^2\frac{\partial^2 \bar{u}}{\partial \bar{y}^2}\right)+\frac{\sigma B^2{}_0}{\rho}\left(-u-\lambda_1 v\frac{\partial u}{\partial y}\right). \tag{21}$$

To get the simulation of the modeled governing equations one need to transform the governing equations by using appropriate similarity transformation given as,

$$\left.\begin{array}{l} \bar{x}=x\sqrt{\dfrac{\nu}{c}},\quad \bar{y}=y\sqrt{\dfrac{\nu}{c}},\quad \bar{u}=u\sqrt{c\nu},\quad \bar{v}=v\sqrt{c\nu}, \\ \bar{T}=T,\quad T_w=\Delta T+T_\infty,\quad p=\rho c\nu P \end{array}\right\}. \tag{22}$$

Eq. (21) in dimensionless from takes the form given as,

$$\left(u\frac{\partial u}{\partial x}+v\frac{\partial u}{\partial y}\right)=-\frac{\partial P}{\partial x}+\beta\left(\frac{\partial u}{\partial y}\frac{\partial P}{\partial y}\right)+\left(\frac{\partial^2 u}{\partial y^2}\right)-\beta\left(u^2\frac{\partial^2 u}{\partial x^2}+2uv\frac{\partial^2 u}{\partial x\partial y}+v^2\frac{\partial^2 u}{\partial y^2}\right).$$
$$+M^2\left(-u-\lambda_1 c\nu\frac{\partial u}{\partial y}\right). \tag{23}$$

Boundary conditions take the form given as,

$$u=x,\quad v=0\quad \text{at}\quad y=0, \tag{24}$$

$$u=\frac{a}{c}x+\frac{b}{c}y,\qquad \text{as}\quad y\to\infty. \tag{25}$$

Now, for heat transfer analysis, assume that T_∞ is the temperature of the fluid while the temperature of the stretching surface is represented by T_w. By using the transformation given in Eq. (22) and Eq. (4), Eq. (3) becomes,

$$u\frac{\partial T}{\partial x}+v\frac{\partial T}{\partial y}=\frac{1}{Pr}\frac{\partial}{\partial y}\left(\left(1+\frac{4}{3}Rd\left(\left(\theta_w-1\right)T+1\right)^3\right)\frac{\partial T}{\partial y}\right). \tag{26}$$

The boundary conditions become,

$$\left.\begin{array}{lll} T=1 & \text{at} & y=0, \\ T=0 & \text{as} & y\to\infty \end{array}\right\} \tag{27}$$

where $\beta=\lambda_1 c$ is Deborah number which represents the fluidity of the material, $Pr=\mu c_p/k$ is the Prandtl number, $M^2=\sigma B_0^2/\rho$ is the Hartmann number, $Rd=4\sigma^* T_\infty^3/k\left(\alpha_r+\sigma_s\right)$ and $\theta_w=T_w/T_\infty$ represents the temperature of the surface same used by Ghaffari et al. (2016). The stream function ψ that will be used in the governing equations, as shown below,

$$u=\frac{\partial \psi}{\partial y}\ ,\quad v=-\frac{\partial \psi}{\partial x}. \tag{28}$$

Using Eq. (28) in (23) to (27), one can have,

$$\frac{\partial\psi}{\partial y}\frac{\partial^2\psi}{\partial x\partial y}-\frac{\partial\psi}{\partial x}\frac{\partial^2\psi}{\partial y^2}+\beta\left(\left(\frac{\partial\psi}{\partial y}\right)^2\frac{\partial^3\psi}{\partial y^3}-2\frac{\partial\psi}{\partial y}\frac{\partial\psi}{\partial x}\frac{\partial^3\psi}{\partial x\partial y^2}+\left(\frac{\partial\psi}{\partial x}\right)^2\frac{\partial^3\psi}{\partial x^2\partial y}\right)=-\frac{\partial P}{\partial x}+$$

$$\beta\left(\frac{\partial^2\psi}{\partial y^2}\frac{\partial P}{\partial y}\right)+\left(\frac{\partial^3\psi}{\partial y^3}\right)+M^2\left(-\frac{\partial\psi}{\partial y}+\beta\frac{\partial\psi}{\partial x}\frac{\partial^2\psi}{\partial y^2}\right), \tag{29}$$

$$\left(\frac{\partial\psi}{\partial y}\frac{\partial T}{\partial x}-\frac{\partial\psi}{\partial x}\frac{\partial T}{\partial y}\right)=\frac{1}{Pr}\frac{\partial}{\partial y}\left(\left(1+\frac{4}{3}Rd\left(\left(\theta_w-1\right)T+1\right)^3\right)\frac{\partial T}{\partial y}\right), \tag{30}$$

$$\psi=0,\quad \frac{\partial\psi}{\partial y}=x,\quad T=1\quad \text{at}\quad y=0,$$

$$\psi=0,\quad \frac{\partial\psi}{\partial y}=x,\quad T=1\quad \text{at}\quad y=0\ , \tag{31}$$

$$\psi=\frac{a}{c}xy+\frac{1}{2}\gamma y,\quad T=0\quad \text{as}\quad y\to\infty. \tag{32}$$

where $\gamma=b/c$ denotes shear in the free stream of the flow. Suppose the solution of Eqs. (29) and (30) subject to boundary conditions Eq. (31) and (32) is of the form,

$$\psi=x\tilde{f}(y)+\tilde{g}(y),\quad T=\tilde{\theta}(y). \tag{33}$$

The functions $\tilde{f}(y)$ and $\tilde{g}(y)$ are the oblique and normal elements of the streams. Using Eq. (33) in Eqs. (29) to (32) we have,

$$\left(x\tilde{f}'(y)+\tilde{g}'(y)\right)\tilde{f}'(y)-\tilde{f}(y)\left(x\tilde{f}''(y)+\tilde{g}''(y)\right)+\beta\left(\left(\tilde{f}(y)\right)^2\left(x\tilde{f}'''(y)+\tilde{g}'''(y)\right)\right)$$

$$-2\tilde{f}(y)\left(x\tilde{f}'(y)+\tilde{g}'(y)\tilde{f}''(y)\right)=-\frac{\partial P}{\partial x}+\beta\left(x\tilde{f}''(y)+\tilde{g}''(y)\right)\frac{\partial P}{\partial y}+x\tilde{f}'''(y)+\tilde{g}'''(y)$$

$$+M^2\left(-\left(x\tilde{f}'(y)+\tilde{g}'(y)\right)+\beta\tilde{f}(y)\left(x\tilde{f}''(y)+\tilde{g}''(y)\right)\right), \tag{34}$$

$$\frac{\partial}{\partial y}\left(\left(1+\frac{4}{3}Rd\left(\left(\theta_w-1\right)\tilde{\theta}+1\right)^3\right)\tilde{\theta}'\right)+Pr\tilde{f}(y)\tilde{\theta}'=0, \tag{35}$$

$$\tilde{f}(y)=0,\quad \tilde{f}'(y)=1,\quad \tilde{g}(y)=0,\quad \tilde{g}'(y)=0,\quad \tilde{\theta}(y)=1\quad \text{at}\quad y=0, \tag{36}$$

$$\tilde{f}'(y)=\frac{a}{c},\quad \tilde{g}'(y)=\gamma y,\quad \tilde{\theta}(y)=0,\quad \text{as}\quad y\to\infty. \tag{37}$$

After eliminating the pressure from Eq. (34), it takes the form as follows,

$$\left(x\tilde{f}'(y)+\tilde{g}'(y)\right)\tilde{f}'(y)-\tilde{f}(y)\left(x\tilde{f}''(y)+\tilde{g}''(y)\right)$$

$$+\beta\left(\left(\tilde{f}(y)\right)^2\left(x\tilde{f}'''(y)+\tilde{g}'''(y)\right)-2\tilde{f}(y)\left(x\tilde{f}'(y)+\tilde{g}'(y)\tilde{f}''(y)\right)\right)$$

$$=-A\gamma+x\left(\frac{a}{c}\right)^2+x\tilde{f}'''(y)+\tilde{g}'''(y)+M^2\left(\frac{a}{c}\right)x$$

$$+M^2\left(-\left(x\tilde{f}'(y)+\tilde{g}'(y)\right)+\beta\tilde{f}(y)\left(x\tilde{f}''(y)+\tilde{g}''(y)\right)\right). \tag{38}$$

Now by comparing the coefficient as x^1 and x^0 in Eq. (38), one can have,

$$\tilde{f}''' + \left(\frac{a}{c}\right)^2 - \tilde{f}'^2 + \tilde{f}\tilde{f}'' - \beta\left(\tilde{f}^2\tilde{f}''' - 2\tilde{f}\tilde{f}'\tilde{f}'' - M^2\tilde{f}\tilde{f}''\right) + \left(\frac{a}{c}\right)M^2 - M^2\tilde{f}' = 0, \tag{39}$$

$$\tilde{g}''' + \tilde{g}''\tilde{f} - \tilde{g}'\tilde{f}' - \beta\left(\tilde{f}^2\tilde{g}''' - 2\tilde{f}\tilde{g}'\tilde{f}'' - M^2\tilde{g}''\tilde{f}\right) - M^2\tilde{g}' = A\gamma, \tag{40}$$

where boundary layer displacement is represented by A. Now for more simplification using a new variable is introduced which is defined as,

$$\tilde{g}'(y) = \gamma\tilde{h}(y). \tag{41}$$

Eq. (38) and the associated boundary condition are reduced to,

$$\tilde{h}'' + \tilde{h}'\tilde{f} - \tilde{h}\tilde{f}' - \beta\left(\tilde{f}^2\tilde{h}'' - 2\tilde{f}\tilde{h}\tilde{f}'' - M^2\tilde{h}'\tilde{f}\right) - M^2\tilde{h} = A, \tag{42}$$

$$\tilde{h}(y) = 0 \quad \text{at} \quad y = 0, \tag{43}$$

$$\tilde{h}'(y) = 1 \quad \text{as} \quad y \to \infty. \tag{44}$$

The local Nusselt number of physical quantities is defined below as,

$$Nu_x = \frac{\bar{x}\, q_w}{k\left(T_w - T_\infty\right)}, \tag{45}$$

where,

$$q_w = -\left[\left(\frac{4}{3}\frac{4\sigma^*\bar{T}^3}{\left(\alpha_r + \sigma_s\right)} + k\right)\frac{\partial\bar{T}}{\partial\bar{y}}\right]. \tag{46}$$

Using dimensionless variables and transformation given in Eq. (22) the above equation reduces to,

$$Nu_x\left(Re_x\right)^{\frac{-1}{2}} = -\left[\left(\frac{4}{3}Rd\left(\theta_w\right)^3 + 1\right)\tilde{\theta}'\right]. \tag{47}$$

It is worth mention here that limiting case for Newtonian case can be obtained by placing $\beta = 0$ and case orthogonal stagnation point flow can also be obtained by placing $\gamma = 0$.

3. Numerical Solution

Using the boundary condition (36), (37), (43), and (44) in the non-linear equation of (35), (39), and (42). They solve these equations in numerical with the parallel shooting method. The simple shooting method is very easy in the compare of parallel shooting method, but the simple shooting method is very difficult to solve higher non-linear problems. That way we used parallel shooting as presented by Shi et al. (2021). The parallel method of shooting is well-organized. The technique is described below:

Equations (35), (39) and (42) are reduced to the first order of differential equations by letting $\tilde{f} = f_1$ $h = f_4$, $\tilde{h}' = f_5$, and $\tilde{\theta} = f_6$.

$f_1' = f_2$, $f_2' = f_3$,

$$f_3' = \frac{1}{1 - \beta f_1^2}\left(f_2^2 - \left(\frac{a}{c}\right)^2 - f_1 f_3 - \beta\left(2\beta f_1 f_2 f_3 + M^2 f_1 f_3\right) - \left(\frac{a}{c}\right)M^2 + M^2 f_2\right), \tag{47}$$

$$f_4^{'} = f_5,$$
$$f_5^{'} = \frac{1}{1-\beta f_1^{\,2}}\left(-f_1\, f_5 - \beta\left(2 f_1\, f_3\, f_4 + \sigma B_0^{\,2} f_1\, f_5\right) + \sigma B_0^{\,2} f_4 + A\right), \tag{48}$$
$$f_6^{'} = f_7,$$
$$f_7^{'} = \frac{1}{1+\frac{4}{3}Rd\left(1+(\theta_w-1)\, f_6\right)^3}\left(\left(-4Rd\,(\theta_w-1)\left(1+(\theta_w-1)\, f_6\right)^2\right)(f_7)^2 - Prf_1 f_7\right). \tag{49}$$

The boundary conditions are given below,

$$f_1(0)=0,\ f_2(0)=1,\ f_2(y_\infty)=\frac{a}{c}, \tag{50}$$
$$f_4(0)=0,\ f_5(y_\infty)=1. \tag{51}$$

The considered domain from 0 to y_∞ is divided into the $'n'$ number of intervals where $'n'$ depends strictly on the required convergence of the solution. The problem is solved for the first interval by setting suitable initial guess and the obtained solution is considered as an initial guess for next interval and this process is carried out until the solution for the last interval is obtained. The solution for each interval is obtained such that it satisfies the boundary condition at y_∞. The algorithm is self-developed in MATLAB R2015a.

4. Validation

To present the accuracy of our present computed results the comparison of $f^{''}(0)$ and $h^{'}(0)$ has been made with Pop [32] and Javed and Ghaffari [10] which includes the results for Newtonian and non-Newtonian Maxwell fluid given in **Table (1)**. It is found that our present computed results are highly convergent with Pop [32] and Javed and Ghaffari [10] It is clear from the table that the value of $f^{''}(0)$ is increases as we enhance the value of a/c but $h^{'}(0)$ increases at a certain value and then decreased.

5. Results and Discussion

Eqs. (35), (39) and (42) with appropriate conditions given in Eqs. (36), (37), (43) and (44) have been solved by implementing above mentioned scheme for various values of involved parameters $\beta, a/c,\ \gamma$ and M. Figures (2a) to (2d) are plotted to present the variation of horizontal velocity u for various values of velocities ratio a/c with fixed values of $x,\ \ \beta, M,\ \gamma = 0.0, 0.5, 1.0$ and 5.0 It is seen that the velocity u increase with enhancement of γ. The Figure (2a) represents the orthogonal flow i.e., $\gamma = 1.0$, whereas Figure (2b) to (2d) shows the non-orthogonal stagnation point flow $(\gamma \neq 0)$. It is observed from the figures that there exist two boundary layer structures which depend upon the ratio of straining and stretching velocities. It is seen that when $a/c > 1$ the flow has normal boundary layer structure but when $a/c < 1$ then the structure shows inverted behavior which is same as reported by Javed and Ghaffari [10]. It is also noted that the thickness of boundary layer decreases as we increase the value of a/c. It is also seen that there exists no boundary layer when $a/c=1$its means that viscous effects near the boundary vanishes when both shearing and straining velocities are equal. This behavior is same for both orthogonal and non-orthogonal stagnation point flows. The Figures (2a) to (2d) show that velocity increases as there is an increase in value of γ. Figure (3a) and (3b) is plotted to examine the variational effects of Deborah number β for orthogonal flow $(\gamma=0)$ and non-orthogonal flow $(\gamma=1.0)$ with a fixed value of M on horizontal velocity u. It is seen that by increasing the value of β figures show that for the inverted boundary layer, the horizontal velocity decreases and thickness of boundary layer decrease but for normal boundary layer the velocity increases and thickness increases for both $\gamma=0$ and $\gamma=1$. Figures (4a) and (4b) shows the variational effects of magnetic field on the orthogonal stagnation point flow and non-orthogonal point flow respectively for fixed values of β. It is clear from the figures that by enhancing the magnetic field the horizontal velocity decreases, but the boundary layer becomes thinner for an inverted boundary and for the normal boundary layer, the horizontal velocity u increases and the boundary layer thickness decreases. The Deborah number (De) is a dimensionless number, often used in rheology to characterize the fluidity of materials under specific flow conditions. It quantifies the observation that given enough time even a solid-like material might flow, or a fluid-like material can act solid when it is deformed rapidly enough.

Figure (5) shows that the horizontal velocity decreased when the value of β is enhanced by keeping the other parameters fixed. The enhancement in the strength of the applied magnetic field dominates the electromagnetic forces in comparison to the viscous forces which retards the motion of the flow. Therefore, successive decrement in the magnitude of axial velocity in the center of the channel is addressed by incrementing the value of magnetic parameter M, whereas one can see the counter behavior of the fluid’s velocity near the boundary. Figure (6) is designed to examine the effects of varying M on horizontal velocity for fixed values of $\gamma, a/c$ and β. Same behavior is observed as that was in the case of effects of β but a minor decrease is observed for $M=1$ and 2. Figures (7a) and (7b) shows the streamlines for oblique flow for $a/c=0.5$ (dashed lines) and 5.0 (solid lines) with fixed $\beta=4, M=2.0$ and $\gamma=0.2$ and 2.0, It is seen that by increasing stretching velocity the streamlines symmetry of the flow disturbs and lines get more tilted towards left due to increase in straining velocity for $\gamma=2.0$ but there is no tilted behavior is seen for $\gamma=0.2$ and flow becomes symmetric.

Figure (8a) and (8b) shows streamlines for oblique flow, for $\gamma=-10$ and -30 (dashed lines) and 10 and 30 (solid lines) with fixed $\beta=4, M=2.0$ nd $a/c=0.5$. It is seen that by increasing the value of $|\gamma|$results in more obliqueness consequently causes the disturbance in the symmetry of the flow.

Figure (9) is plotted to represent the effects of θ_w for various values of θ_w with fixed values of $\beta, M, \gamma, a/c, \Pr$ and Rd. It is seen that the temperature of fluid increases rapidly by increasing the value of surface temperature. A concave curve is seen at $\theta_w = 2.0$. Figure (10) is designed to elaborate the effects of Prandal number with fixed values of $\beta = 0.2, M = 1.0, \gamma = 5.0, a/c = 0.2,$ $Rd = 2.0$ and $\theta_w = 2.0$. It is observed from the figure that the enhancement in the Prandtl number results in a decrease in the value of temperature of flow. This figure demonstrates that the increase of Prandtl number which consequently decreases of thermal conductivity that results in decrease of temperature distribution which tend to zero as the space variable η increase from the wall and hence thermal boundary layer thickness decreases as Prandtl number $\Pr$ increases. Near the boundary the thermal boundary layer thickness is higher. Figure (11) shows the effects of radiation parameter $Rd,$ with fixed values of $\beta = 0.2, M = 1.0, \gamma = 5.0, a/c = 2.0, \Pr = 0.05$ and $\theta_w = 2.0$ It is observed the by increasing the values of Rd the temperature of flow increases; also, concave curves are observed for $Rd = 5$ and 10.

6. Closing Remarks

The stretching surface is surrounded by a small band of static fluid layer known as the boundary layer. How quickly fluids and energy are transferred from the surface to the surrounding fluid depends on the thickness of the boundary layer. The amount of heat, energy, and fluid that a layer releases into the system can be decreased by a thick boundary layer. The influence of Hartmann number and radiation parameter on the boundary layer flow of Maxwell fluid in the region of oblique stagnation point over linear symmetrically stretching sheet is investigated. The participation of the involved parameters is studied by plotting their different variation through graphs and tables. This study concludes increase in the parameter a/c decreases the boundary layer thick of oblique stagnation point flow of non-Newtonian fluid while radiation parameter and surface heating parameter increase the thermal boundary layer thickness. By increasing the value of Deborah number for inverted boundary layer, the horizontal velocity decreases, and thickness of boundary layer decreases. It is also noted that enhancing the strength of magnetic field, the horizontal velocity decreases but boundary layer becomes thinner. Streamlines shows that increasing the value of $|\gamma|$ results in more obliqueness. Temperature of fluid increases rapidly by increasing the value of surface temperature and radiation parameter but decreases by increasing the Prandtl number. The boundary layer flow of oblique stagnation point flow disturbs the symmetry of the flow.

Nomenclature:

μ	Absorption coefficient	E	Activation energy
T_∞	Ambient temperature	A	Boundary layer displacement

b	Body forces	k	Boltzmann constant
x, y	Cartesian coordinates	σ	Chemical rate constant
β	Deborah number	μ	Dynamic viscosity
ρ	Density of fluid	θ	Dimensionless temperature
C	Dimensional constant	T_∞	Fluid temperature
$\bar{A}_1$	First tensor by Rivlin Ericksen	a	Fluid velocity
M	Hartmann number	ν	Kinematic viscosity
∇^2	Laplacian operator	B	Magnetic field vector
$\tilde{g}(y)$	Normal element of the streams	Nu_x	Nusselt number
$\tilde{f}(y)$	Oblique element of the streams	$\Pr$	Prandtl number
P	Pressure of fluid	Rd	Radiation parameter
α_r	Roseland definition	q_r	Radiative heat flux
σ_s	Scattering coefficient	ψ	Stream function
S_c	Schmidt number	β_0	Strength of magnetic field
γ	Shear in the free stream of the flow	$\bar{S}$	Stress tensor
η	Similarity variable	c	Stretching constant
c_p	Steady pressure of real heat	T_w	Stretching surface temperature
$\sigma*$	Stefan Boltzmann's-constant	U_w	Stretching velocity of sheet
δ	Temperature relative parameter	φ	Thermal stratification parameter
κ	Thermal conductivity	$\bar{\lambda}_1,$	Time relaxation content
α	Thermal diffusivity	$\bar{L}^T$	Transpose of velocity gradient
$\bar{L}$	Velocity gradient	u, v	Velocity components
$\bar{V}$	Velocity vector	T_w	Wall temperature
θ_w	Wall temperature	λ	Weissenberg number

Table 1: Numerical values of $f''(0)$ and $h'(0)$ for the different values of β and a/c

	Newtonian Fluid $(\beta = 0.0)$			Non-Newtonian Fluid $(\beta = 0.2)$				
	Pop [32]	Javed and Ghaffari [10]	Present Results	Pop (2004)	Javed and Ghaffari [10]	Present Results	Javed and Ghaffari [10]	Present Results
a/c	$f''(0)$	$f''(0)$	$f''(0)$	$f''(0)$	$f''(0)$	$f''(0)$	$h'(0)$	$h'(0)$
0.01	-0.9981	-0.99802	-0.9980	-1.0499	-1.05009	-1.0500	-0.51368	-0.5137
0.02	-0.9958	-0.99579	-0.9957	-10476	-1.04778	-1.0477	-0.24667	-0.2467
0.05	-0.9876	-0.98758	-0.9875	-1.0393	-1.03939	-1.0394	0.07239	0.0724
0.10	-0.9694	-0.96939	-0.9693	-1.0207	-1.02082	-1.0208	0.28154	0.2815
0.20	-0.9181	-0.91811	-0.9181	-0.96823	-0.96823	-0.9683	0.49218	0.4922
0.50	-0.6673	-0.66726	-0.6672	-0.70779	-0.70779	-0.7077	0.79610	0.7961
1.00	0.0000	0.0000	0.0000	0.0000	0.0000	0.0000	1.0000	1.0000
2.00	2.0175	2.01749	2.0175	2.2225	2.22314	2.2231	1.09213	1.0921
3.00	4.7294	4.72824	4.7294	5.3544	5.35217	5.3522	0.78434	0.7843
5.00	11.7537	11.75190	11.7534	14.0144	17.00169	17.0017	-2.04649	-2.0465
10.0	36.2689	36.25704	36.2699	48.3354	48.33540	48.3354	-2.34185	-2.3419

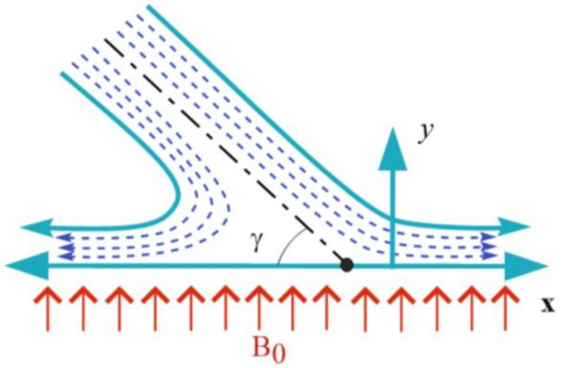

Figure 1: Geometry of the considered physical plane

302

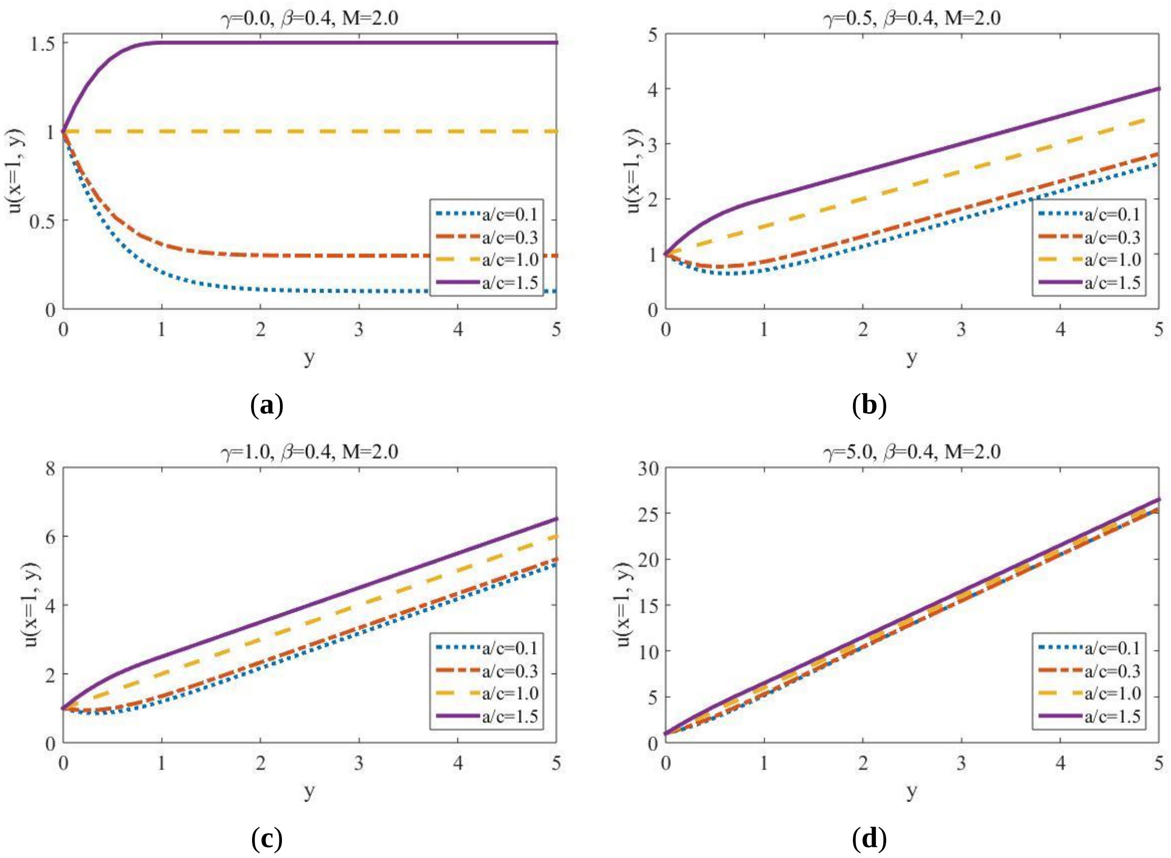

Figure 2. Graph of variation of horizontal velocity u along $y-$axis at $x=1$ for various values of a/c and $\beta=0.4$ and $M=2.0$ with **(a)** $\gamma=0.0$ **(b)** $\gamma=0.5$ **(c)** $\gamma=1.0$ **(d)** $\gamma=5.0$

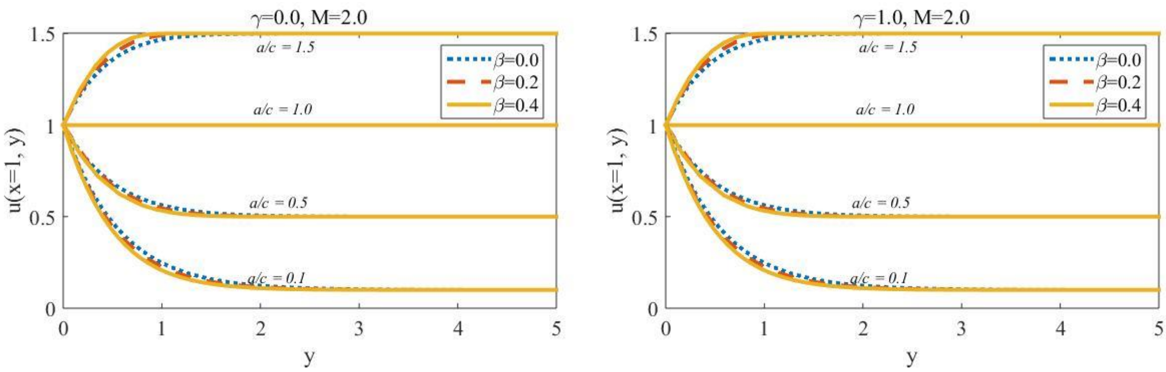

(**a**) (**b**)

Figure 3. Graph of variation of horizontal velocity u along $y-$axis at $x=1$ for various values of β and $a/c=0.1, 0.5, 1.0$ and 1.5 and $M=2.0$ with **(a)** $\gamma=0.0$ (orthogonal flow) **(b)** $\gamma=1.0$ (non-orthogonal flow)

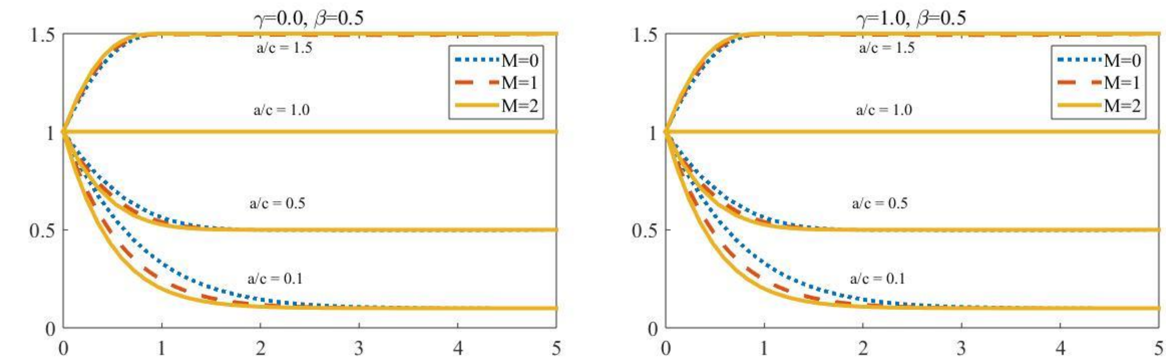

(**a**) (**b**)

Figure 4. Graph of variation of horizontal velocity u along $y-$axis at $x=1$ for various values of M when $a/c=0.1, 0.5, 1.0$ and 1.5 and $\beta=0.5$ with **(a)** $\gamma=0.0$ (orthogonal flow) **(b)** $\gamma=1.0$ (non-orthogonal flow)

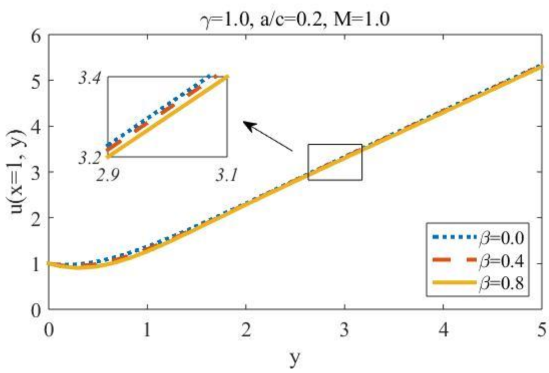

Figure 5. Graph of variation of horizontal velocity u along $y-$axis at $x=1$ for various values of β with fixed $a/c=0.2$ and $M=1.0$ for $\lambda=1.0$ (non-orthogonal flow)

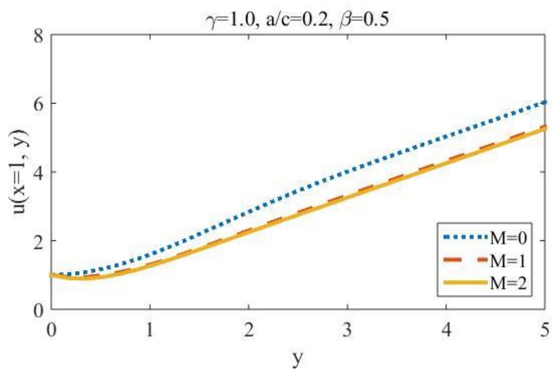

Figure 6. Graph of variation of horizontal velocity u along $y-$axis at $x=1$ for various values of M with fixed $a/c=0.2$ and $\beta=0.5$ for $\lambda=1.0$ (non-orthogonal flow)

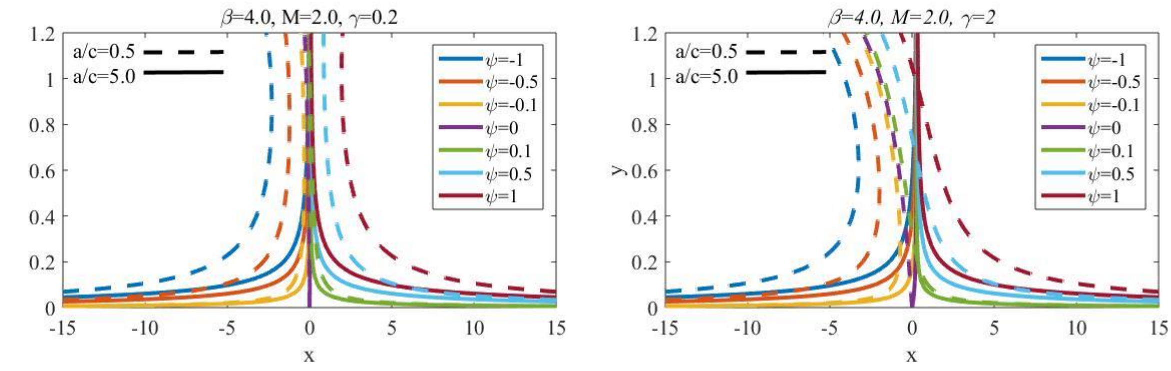

(a) **(b)**

Figure 7. Graph of streamlines for oblique flow, for $a/c = 0.5$ (dashed lines) and 5.0 (solid lines) with fixed $\beta = 4, M = 2.0$ with **(a)** $\gamma = 0.2$ and **(b)** $\gamma = 2.0$

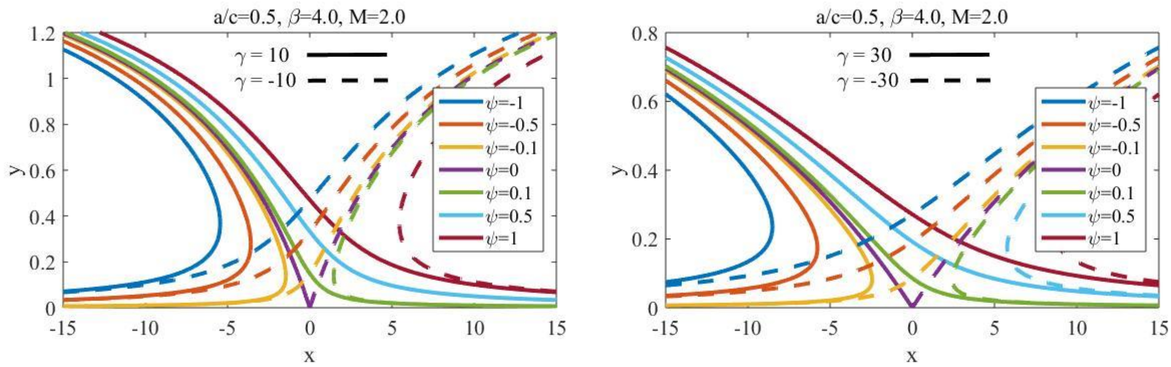

(a) **(b)**

Figure 8. Graph of streamlines for oblique flow, for fixed $\beta = 4, M = 2.0$ and $a/c = 0.5$ with **(a)** $\gamma = -10$ (dashed lines) and 10 (solid lines) and **(b)** $\gamma = -30$ (dashed lines) and 30 (solid lines)

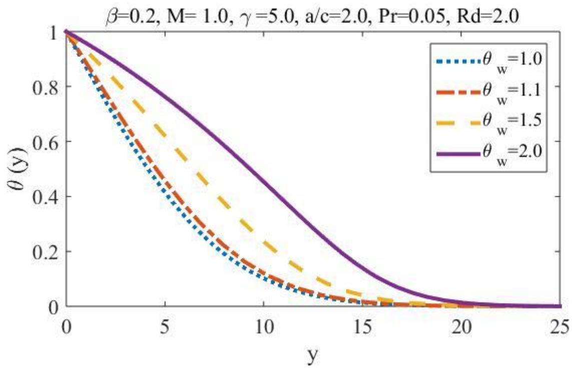

Figure 9. Graph of variation of θ for various values of θ_w with fixed $\beta = 0.2, M = 1.0,$ $\gamma = 5.0, a/c = 2.0, Rd = 2.0, \Pr = 0.05$ and $Rd = 2.0$

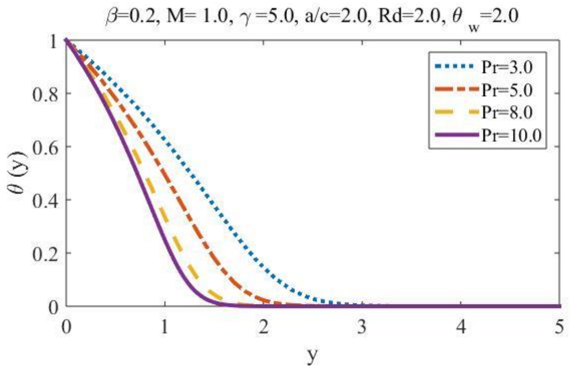

Figure 10. Graph of variation of θ for various values of Pr with fixed $\beta = 0.2, M = 1.0,$ $\gamma = 5.0, a/c = 2.0, Rd = 2.0, Rd = 2.0$ and $\theta_w = 2.0$

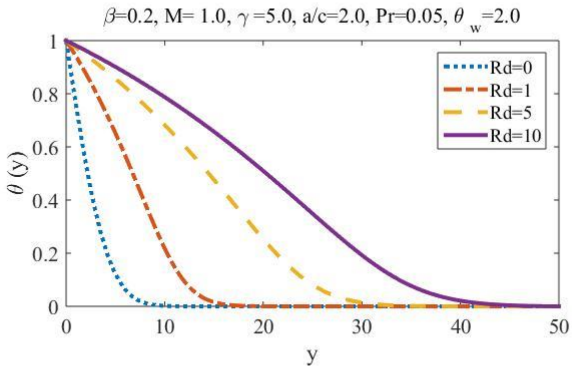

Figure 11. Graph of variation of θ for various values of Rd with fixed $\beta = 0.2, M = 1.0, \gamma = 5.0, a/c = 2.0, \mathrm{Pr} = 0.05$ and $\theta_w = 2.0$

References

[1] Stuart, J. T. "The viscous flow near a stagnation point when the external flow has uniform vorticity". *Journal of the Aerospace Sciences*, **26**(2), pp. 124-125 (1959).

[2] Tamada, K. "Two-dimensional stagnation-point flow impinging obliquely on a plane wall". *Journal of the Physical Society of Japan*, **46**(1), pp. 310-311 (1979).

[3] Dorrepaal, J. M. "An exact solution of the Navier-Stokes equation which describes non-orthogonal stagnation-point flow in two dimensions" *Journal of Fluid Mechanics*, **163**, pp. 141-147. (1986).

[4] Tooke, R. M., & Blyth, M. G. "A note on oblique stagnation-point flow". *Physics of Fluids*, **20**(3) (2008).

[5] Husain, I., Labropulu, F., and Pop, I. "Two-dimensional oblique stagnation-point flow towards a stretching surface in a viscoelastic fluid" *Central European Journal of Physics*, **9**(1), pp. 176-182 (2011).

[6] Wang, S., & Tan, W. "Stability analysis of Soret-driven double-diffusive convection of Maxwell fluid in a porous medium". *International Journal of Heat and Fluid Flow*, **32**(1), pp. 88-94 (2011).

[7] Mukhopadhyay, S. “Heat transfer analysis of the unsteady flow of a Maxwell fluid over a stretching surface in the presence of a heat source/sink”. *Chinese Physics Letters*, **29**(5), pp. 054703 (2012).

[8] Nadeem, S., Haq, R. U., and Khan, Z. H. “Numerical study of MHD boundary layer flow of a Maxwell fluid past a stretching sheet in the presence of nanoparticles”. *Journal of the Taiwan Institute of Chemical Engineers*, **45**(1), pp. 121-126 (2014).

[9] Sajid, M., Ahmed, B., & Abbas, Z. “Steady mixed convection stagnation point flow of MHD Oldroyd-B fluid over a stretching sheet”. *Journal of the Egyptian Mathematical Society*, **23**(2), pp. 440-444. (2015).

[10] Javed, T., and Ghaffari, A. “Numerical study of non-Newtonian Maxwell fluid in the region of oblique stagnation point flow over a stretching sheet” *Journal of Mechanics*, **32**(2), pp. 175-184 (2016).

[11] Javed, T., Ahmad, H., & Ghaffari, A. “Mixed convection boundary-layer flow of a viscoelastic fluid due to horizontal elliptic cylinder with constant heat flux” *Thermal Science*, **22**(1 Part B), pp. 519-531 (2018).

[12] Sajid, M., Sadiq, M. N., Mahmood, K., et al. “A Legendre wavelet spectral collocation method for analysis of thermal radiation and slip in the oblique stagnation-point flow of Walters-B liquid towards a stretching surface”. *Sādhanā*, **44**(6), pp.136 (2019).

[13] Khan, M., Malik, M. Y., Salahuddin, T.et al. “Generalized diffusion effects on Maxwell nanofluid stagnation point flow over a stretchable sheet with slip conditions and chemical reaction”. *Journal of the Brazilian Society of Mechanical Sciences and Engineering,* **41**(3), pp. 138 (2019).

[14] Jawad, M., Shah, Z., Islam, S., et al. “Impact of nonlinear thermal radiation and the viscous dissipation effect on the unsteady three-dimensional rotating flow of single-wall carbon nanotubes with aqueous suspensions”. *Symmetry*, **11**(2), pp. 207 (2019).

[15] Majeed, A., Zeeshan, A., Noori, F. M., et al. “Influence of rotating magnetic field on Maxwell saturated ferrofluid flow over a heated stretching sheet with heat generation/absorption”. *Mechanics & Industry*, **20**(5), pp. 502 (2019).

[16] Mahmood, Khalid, Muhammad Noveel Sadiq, Muhammad Sajid, et al. "Heat transfer in stagnation-point flow of a Jeffrey fluid past a lubricated surface." *Journal of the Brazilian Society of Mechanical Sciences and Engineering* **41** pp. 1-9 (2019).

[17] Alizadeh, R., Karimi, N., & Nourbakhsh, A. “Effects of radiation and magnetic field on mixed convection stagnation-point flow over a cylinder in a porous medium under local thermal non-equilibrium”. *Journal of Thermal Analysis and Calorimetry*, **140**, pp. 1371-1391 (2020).

[18] Reza-E-Rabbi, S., Ahmed, S. F., Arifuzzaman, S. M., et al. “Computational modelling of multiphase fluid flow behaviour over a stretching sheet in the presence of nanoparti-

cles”. *Engineering Science and Technology, an International Journal*, **23**(3), pp. 605-617 (2020).

[19] Khan, N., Nabwey, H. A., Hashmi, M. S., et al. “A theoretical analysis for mixed convection flow of Maxwell fluid between two infinite isothermal stretching disks with heat source/sink”. *Symmetry*, **12**(1), 62 (2020).

[20] Ibrahim, W., & Negera, M. “MHD slip flow of upper-convected Maxwell nanofluid over a stretching sheet with chemical reaction”. *Journal of the Egyptian Mathematical Society*, **28**(1), pp. 7. (2020).

[21] Mekheimer, K. S., & Ramadan, S. F. “New insight into gyrotactic microorganisms for bio-thermal convection of Prandtl nanofluid over a stretching/shrinking permeable sheet”. *SN Applied Sciences*, **2**(3), pp. 450 (2020).

[22] Chu, Y. M., Rehman, M. I. U., Khan, et al. “Transportation of heat and mass transport in hydromagnetic stagnation point flow of Carreau nanomaterial: Dual simulations through Runge-Kutta Fehlberg technique” I*nternational Communications in Heat and Mass Transfer*, **118**, 104858. (2020).

[23] Khan, M. I., Nigar, M., Hayat, T., et al. “On the numerical simulation of stagnation point flow of non-Newtonian fluid (Carreau fluid) with Cattaneo-Christov heat flux”. *Computer Methods and Programs in Biomedicine*, **187**, 105221 (2020).

[24] Mathew, A., Areekara, S., Sabu, A. S., et al. “Significance of multiple slip and nanoparticle shape on stagnation point flow of silver-blood nanofluid in the presence of induced magnetic field”. *Surfaces and Interfaces*, **25**, (2021).

[25] Turkyilmazoglu, M. “Stagnation-point flow and heat transfer over stretchable plates and cylinders with an oncoming flow: Exact solutions”. *Chemical Engineering Science*, **238**, pp. 116596 (2021).

[26] Zaher, A. Z., Ali, K. K., & Mekheimer, K. S. “Electroosmosis forces EOF driven boundary layer flow for a non-Newtonian fluid with planktonic microorganism: Darcy Forchheimer model”. *International Journal of Numerical Methods for Heat & Fluid Flow*, **31**(8), pp. 2534-2559 (2021).

[27] Abbasi, A., Gulzar, S., Mabood, F., et al. “Nonlinear thermal radiation and activation energy features in axisymmetric rotational stagnation point flow of hybrid nanofluid”. *International Communications in Heat and Mass Transfer*, **126**, (2021).

[28] Wahid, N. S., Arifin, N. M., Pop, I., et al. “MHD stagnation-point flow of nanofluid due to a shrinking sheet with melting, viscous dissipation and Joule heating effects”. *Alexandria Engineering Journal*, **61**(12), pp. 12661-12672 (2022).

[29] Reddy, Y. D., Goud, B. S., Khan, et al. “Transport properties of a hydromagnetic radiative stagnation point flow of a nanofluid across a stretching surface”. *Case Studies in Thermal Engineering*, **31**, pp.101839 (2022).

[30] Baig, M. N. J., Salamat, N., Duraihem, F. Z., e al.:" Exact Analytical Solutions of Stagnation point flow over a Heated stretching cylinder: A phase flow nanofluid model" *Chinese Journal of Physics*. (2023).

[31] Gadelhak, A. A., Mekheimer, K. S., Seddeek, M. A., et al. "Energy Transport of Williamson Nano-fluid over a Curved Stretching Surface by Means of FDM". *BioNanoScience*, pp. 1-10 (2023).

[32] Pop, S. R., Pop, I., & Grosan, T. "Radiation effects on the flow near the stagnation point of a stretching sheet". *Technische Mechanik-European Journal of Engineering Mechanics*, **25**(2), pp. 100-106 (2005).

Biography

BILAL AHMED

bilalmaths7@yahoo.com +92-333-5761015

During the period 2014-2018, Dr. Bilal joined the International Islamic University Islamabad (PAK) to teach courses related to mathematics and Allama Iqbal Open University, Islamabad (AIOU, PAK) to teach courses related to Physics, where he worked as a visiting faculty member. In 2017, Dr. Bilal was selected as a Senior Research Assistant in the National Research Program for the University (NRPU) by Higher Education of Pakistan (HEC, PAK) for the project entitled "Study of Mixed Convection Flows Inside a Lid Driven Cavity Using Finite Element Method "and producing some the outstanding research articles.

throughout his academic journey, Dr. Bilal imparted his knowledge by teaching various undergraduate and graduate courses in pure and applied mathematics at institutions such as The University of Lahore (UOL, PK), National University of Science and Technology (NUST, PAK), International Islamic University (IIU, PAK), and University of Science and Technology of Fujairah (USTF, UAE). He also conducted courses related to physics at the International Islamic University (IIU, PAK), Allama Iqbal Open University (AIOU, PAK), and the University of Science and Technology (USTF, UAE). Based on his research and academic activities, he has been awarded two times the status of HEC Approved PhD Supervisor in May 2019 and April 2022 for the next three years in the discipline of Physical Sciences from the Higher Education Commission of Pakistan, (HEC. PAK).

Muhammad Noman

Muhammad Noman: rksardarpur@gmail.com +92-302-3531964

Muhammad Noman was born on December 11, 1997 in District Sargodha, Punjab, Pakistan. He completed his MSc & MPhil in mathematics from the University of Lahore, Lahore, Pakistan. He is serving as Lecturer mathematics in University of Lahore Sargodha campus, Pakistan. His research interests are in the field of fluid mechanics.

Aqsa Aslam

Aqsa Aslam: aqsaaslam607@gmail.com +92 314 3353040

Aqsa Aslam was born on December 4, 1999 in District Chaniot, Punjab, Pakistan. She completed her BS, MPhil from The University Of Lahore, Sargodha Campus and pursuing PhD in Mathematics from the University of Lahore, Lahore, Pakistan. She is serving as Lecturer mathematics in University of Lahore Sargodha campus, Pakistan. Her research interests are in the field of fluid mechanics.

Bibliography of Sadia Kanwal

"Sadia Kanwal has established a robust academic foundation, having successfully attained both her Bachelor of Science (BS) and Master of Philosophy (M.Phil) degrees in Mathematics from the University of Lahore, situated in Sargodha, Pakistan. Her academic journey has been marked by a dedicated focus on the intricate domain of Fluid Mechanics, delving into its complexities and nuances. Furthermore, her scholarly pursuits have extended into exploring alternative theories on peristalsis—an area of significant interest within the realm of biological fluid dynamics. Kanwal's profound curiosity and commitment to these subjects signify a passion for uncovering new perspectives and advancing understanding within these specialized fields of study. Her academic trajectory showcases a commitment to academic excellence and a genuine enthusiasm for probing the boundaries of mathematical theory within the realm of fluid dynamics and biological processes."